

Structure of borate glasses from neutron-diffraction experiments

J. Swenson

Department of Physics, Chalmers University of Technology, S-412 96 Gothenburg, Sweden

L. Börjesson

Department of Physics, Royal Institute of Technology, S-100 44 Stockholm, Sweden

W. S. Howells

Rutherford-Appleton Laboratory, Chilton, Didcot OX11 0QX, United Kingdom

(Received 24 March 1995)

Systematic neutron-diffraction experiments have been performed on metal oxide modified borate glasses, $xM_2O-2B_2O_3$ with $M = Ag, Li, Na$, in order to investigate the short- and intermediate-range structure. The short-range order of the boron-oxygen network, involving the first B-O, B-B, and O-O interatomic distances, is found to be almost identical for the silver, lithium, and sodium borates of the same modifier concentration. A detailed analysis of the first peak in the atomic pair correlation function reveals two different B-O nearest-neighbor distances, 1.37 and 1.47 Å, which are attributed to BO_3 and BO_4 groups, respectively. The relative abundance of three and four coordinated borons are determined for variations of the metal oxide content and found to be in accordance with reported nuclear magnetic resonance results. The low momentum transfer (Q) range of the structure factors of the various metal-oxide modified glasses are significantly different, which indicates differences in the structural organization on an intermediate length-scale 5–15 Å. For Ag_2O and Na_2O modifications considerably longer range correlations are observed as compared with pure vitreous B_2O_3 . In contrast, in the case of Li_2O modification no dramatic change of the intermediate-range order is observed. The different behavior is due to differences in the relative topological arrangements of the various borate groups formed, which in turn appears to be related to the size and degree of covalency of the cation and hence to its ability to form bridges between segments of the BO network.

I. INTRODUCTION

The nature and extent of atomic ordering in simple amorphous solids have attracted considerable interest which has accelerated recently. This is partly because of an increase in the technological use of glasses in various applications ranging from photosensitive semiconducting thin films to highly ionically conducting materials for applications in solid-state batteries. It is also part of a general increasing interest in the fundamental properties of disordered materials. Most simple diatomic glasses such as SiO_2 , B_2O_3 , and P_2O_5 can be considered as isotropic and homogeneous on length scales longer than a few tens of angstroms. However, it is well established that there is a considerable ordering on a scale of the few nearest-neighbor interatomic distances. A famous model for the structures of oxide glasses was early described by Zachariasen¹ and Warren *et al.*² They proposed a continuous random network model in which the glass structure is built up by simple well-defined molecularlike units (e.g., SiO_4 tetrahedra, BO_3 triangles) connected together in a random manner through a distribution of dihedral angles. In this model there is no specific ordering beyond the next-nearest neighbors. However, various structural investigations show the presence of a sharp diffraction peak at low momentum transfer Q [the so-called first sharp diffraction peak (FSDP)], which has been interpret-

ed to indicate various kinds of ordering on an intermediate length scale 5–20 Å.^{3–6} The origin of the FSDP and the corresponding structural ordering and related properties are presently subjects of considerable debate.^{5–8}

Krogh-Moe⁹ proposed a structural model specific for $xM_2O-B_2O_3$ glasses in which the network is built up by various structural units that occur in the corresponding crystalline compounds, such as boroxol, tetraborate, and diborate groups. Some of the main features of the Krogh-Moe model for borate glasses are supported by nuclear magnetic resonance^{10–13} (NMR), Raman,^{14,15} and infrared experiments.^{11,16,17} The experiments show that addition of metal oxide to B_2O_3 causes a progressive increase of the number of four-coordinated borons at the expense of three-coordinated ones, changes of the network structures with new types of borate structural groups being formed, and that the metal ions do not participate in the network formation. The coordinations of the metal ions have been investigated by x-ray diffraction^{18,19} and extended x-ray absorption (EXAFS).^{20,21} It was shown that the metal ions mainly coordinate to the negatively charged BO_4 groups. However, it is not clear whether the cations (and the BO_4 groups) tend to cluster into thin pathways suitable for ion diffusion or if they are homogeneously dispersed throughout the glass structure. This problem has been addressed in silicate glasses by computer-simulation tech-

niques²² and experimentally by EXAFS (Ref. 23) and neutron diffraction using isotope substitutions.²⁴

An increasing interest has during recent years been focused on the mechanism of fast ion conductivity in glasses.^{25,26} Most existing models relate the ionic diffusion to some specific structural arrangements, e.g., an open network,^{17,27} clustering,^{28,29} conducting pathways,³⁰ etc. The relatively few experimental studies of the microscopic structures reported so far have concentrated on the local structure, whereas there is a lack of investigations that concern the intermediate-range structure, which involves some of the structural elements of interest in the proposed models. It is the aim of the present neutron-diffraction study to elucidate the structural changes induced by increasing modifier content x , both on the local and the intermediate-range scales, in three binary glass systems $xM_2O-B_2O_3$, where $M = Ag, Li, Na$, respectively. Glasses of these systems exhibit room-temperature ionic conductivities up to 10^{-7} S cm⁻¹ and are therefore of interest as solid electrolytes in solid-state electrochemical devices. Such glasses are also used as host matrices for further dopings with metal-halide salts to achieve dramatically higher conductivities (up to 10^{-2} S cm⁻¹). The present study will then also serve as a basis for further structural studies of the corresponding metal-halide-doped ternary glasses.

The present investigation shows that the short-range boron-oxygen structures are almost identical for the three systems. However, the local coordination of the cations as well as the intermediate-range structural ordering are significantly different for Ag₂O, Li₂O, and Na₂O modified borate glasses.

II. DIFFRACTION NOTATION

We will use the following notation for the scattered neutron intensity from glasses and for the corresponding real-space functions. The quantity measured in a neutron-diffraction experiment is the differential scattering cross section $I(Q)$, where Q is the momentum transfer. The differential scattering cross section $I(Q)$ can also be expressed as a sum of two terms:³¹

$$I(Q) = I_S + I_D = \sum_i \frac{n_i \sigma_i^s}{4\pi} [1 + P_i(Q, \theta)] + \frac{1}{Q} \int_0^\infty D(r) \sin(Qr) dr, \quad (1)$$

where the first term is known as the self-scattering and the second term is known as the distinct scattering. It is the latter which carries information on the interatomic correlations. The summation is taken over the different elements in the sample, n_i is the number of i atoms in the scattering unit, and σ_i^s is the total bound atom scattering cross-section for element i , $D(r)$ is the neutron-weighted reduced pair distribution function, and $P_i(Q, \theta)$ represents inelastic scattering events and is known as the Placzek correction term.³¹ The static structure factor $S(Q)$ is the normalized form of the differential scattering cross section $I(Q)$, i.e.,

$$S(Q) = I(Q) / I_S. \quad (2)$$

$D(r)$ is obtained by Fourier transformation of the distinct scattering;

$$D(r) = \frac{2}{\pi} \int_0^\infty Q I_D(Q) \sin(rQ) dQ. \quad (3)$$

$D(r)$ can also be written as the neutron-weighted (i.e., dependent upon the scattering lengths of the constituent atoms) sum of the reduced partial radial distribution functions $d_{ij}(r)$;

$$D(r) = \sum_{i,j} n_i b_i b_j d_{ij}(r), \quad (4)$$

where b_i is the coherent scattering length for element i .

The more commonly used total atomic pair correlation function $G(r)$ is obtained from $D(r)$ through

$$G(r) = D(r) / 4\pi\rho r \left[\sum_i n_i b_i \right]^2 + 1, \quad (5)$$

where ρ is the atomic number density.

Let us here also define the total correlation function $T(r)$ and the radial distribution function $J(r)$:

$$T(r) = 4\pi\rho r G(r) \quad (6)$$

and

$$J(r) = rT(r), \quad (7)$$

respectively.

III. EXPERIMENTAL DETAILS

Glasses with compositions $xM_2O-B_2O_3$ ($M = Ag, Li, Na$), with $x = 0.125, 0.25, 0.5$ (only $x = 0.5$ for $M = Na$), were prepared using a conventional melt-quenching method according to procedures described previously.^{32,33} For the $0.5M_2O-B_2O_3$ composition an additional sample was prepared with appropriate combination of ⁶Li and ⁷Li to give the zero scattering length of Li. In all samples boron was isotopically enriched in ¹¹B (99%) in order to minimize the influence of the high neutron absorption of ¹⁰B present in natural boron. The samples, which were in shapes of cylindrical rods with a diameter of 9 mm and a length of 50 mm, were mounted in thin-walled vanadium containers. The neutron-diffraction experiments were performed on the time-of-flight Liquid and Amorphous Materials Diffractometer (LAD) at the pulsed neutron source ISIS, Rutherford Appleton Laboratory. The diffractometer has been described in detail elsewhere.³⁴ Time-of-flight spectra were recorded separately for each group of detectors at the angles 150°, 90°, 58°, 35°, 20°, 10°, and 5° and also for monitors in the incident and transmitted beams, respectively.

The data of each detector group were corrected separately for background and container scattering, absorption, multiple scattering, and inelasticity effects and normalized against the scattering of a vanadium rod following the procedure in Ref. 35. The absorption correction required some caution because of the high absorption cross section (about 3×10^{-23} cm² for a neutron wavelength of 1.8 Å). It was checked in three ways. First, the absorption and scattering cross sections were calculated

from the measured wavelength dependence of the fraction of neutrons transmitted by the sample, using the monitors for the incident and transmitted beams. The values for the scattering and absorption cross sections were found to be close to those expected from tabulated values for the combination of elements of the respective compositions. Using the values obtained in the correction procedure, we checked the results in two ways: (i) It was verified that the high- Q part of the structure factor was oscillating around a constant level and (ii) $I_D(Q)$ was Fourier transformed to $D(r)$, the spurious peaks were deleted below the first peak, and then $D(r)$ was Fourier transformed back again to obtain $I_D(Q)$. The back-transformed $I_D(Q)$ was in excellent agreement with the original $I_D(Q)$ (in fact, almost indistinguishable) for all the samples, which showed that appropriate absorption cross-section corrections had been applied.

The corrected individual data sets obtained at each angle were then combined to obtain a large Q range and to improve the statistics. For each data set we only used the Q range that agreed with other data sets in the overlapping Q region. For the samples containing silver, we excluded data obtained for neutron wavelengths $< 0.2 \text{ \AA}$, because of a nuclear resonance absorption of $^{109}\text{Ag}^+$ ions at 0.13 \AA .

The final data set of each sample was Fourier transformed to obtain the total neutron-weighted reduced radial distribution function $D(r)$ or the pair correlation function $G(r)$. In order to reduce termination ripples in the correlation function caused by truncation at a finite maximum Q , Q_{max} , we multiplied the integrand in Eq. (3) with a modification function $M(Q)$:

$$M(Q) = \begin{cases} \frac{\sin(Q\Delta r)}{Q\Delta r} & \text{for } Q < Q_{\text{max}} , \\ 0 & \text{for } Q > Q_{\text{max}} , \end{cases} \quad (8)$$

where $\Delta r = \pi/Q_{\text{max}}$.

The effect of the modification function is to greatly reduce termination ripples, although at the expense of some reduced real-space resolution. Fourier transformation of $M(Q)$ produces a peak function with a full width at half maximum (FWHM) of $5.437/Q_{\text{max}}$, which should be compared to the FWHM of $3.8/Q_{\text{max}}$, produced by Fourier transformation of a step function cutting off at $Q = Q_{\text{max}}$.

IV. RESULTS

In Fig. 1 we present the total structure factors for $x\text{Ag}_2\text{O}-\text{B}_2\text{O}_3$, $x\text{Li}_2\text{O}-\text{B}_2\text{O}_3$, and $0.5\text{Na}_2\text{O}-\text{B}_2\text{O}_3$ for $x = 0.125, 0.25, \text{ and } 0.5$ (only $x = 0.5$ for the Na system) glasses determined in the present study together with the structure factor for pure vitreous B_2O_3 reported by Johnson *et al.*³⁶ Note that the oscillations in $S(Q)$ persist to Q values larger than 25 \AA^{-1} (in fact, they are discernible up to 40 \AA^{-1}) for all the investigated samples. Oscillations in the high- Q part are dominated by short-range correlations, which in the present case indicates that the investigated glasses have well-defined short-range

order within molecularlike structural units of the network. Similar results are found for most network glasses.³⁷ As shown in Fig. 1, the structure factors for all the investigated Ag_2O , Li_2O , and Na_2O modified glasses are very similar for $Q > 5 \text{ \AA}^{-1}$. Thus the short-range order of the BO network does not change dramatically with increasing $M_2\text{O}$ content or with change of cation.

The low Q range ($< 5 \text{ \AA}^{-1}$) of $S(Q)$, which is related to correlations beyond the first-nearest-neighbor distance, is almost identical for pure B_2O_3 and for the lithium borate glasses even for high concentrations of Li_2O [see Fig. 1(b)]. In contrast, in the case of Ag_2O modification

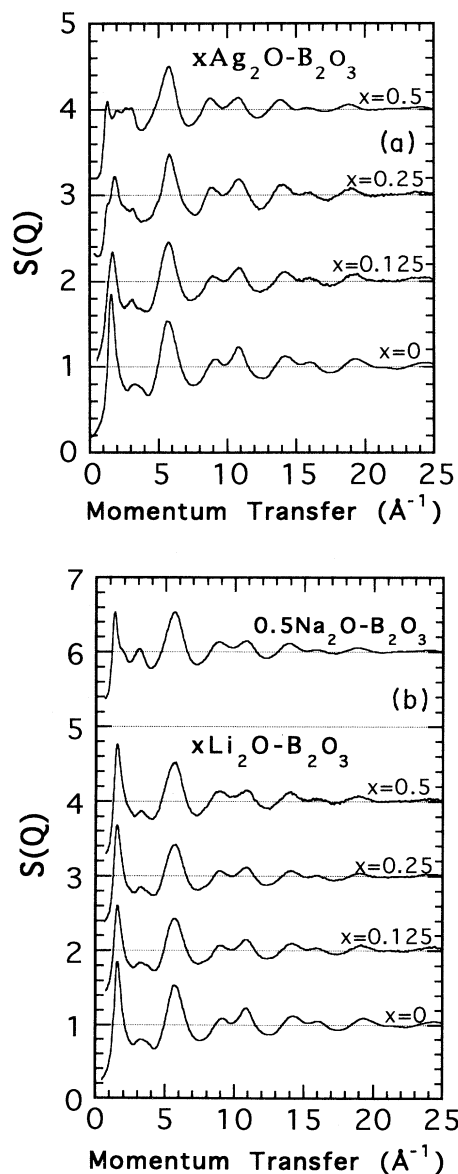


FIG. 1. Structure factors for (a) $x\text{Ag}_2\text{O}-\text{B}_2\text{O}_3$ and (b) $0.5\text{Na}_2\text{O}-\text{B}_2\text{O}_3$ and $x\text{Li}_2\text{O}-\text{B}_2\text{O}_3$ glasses. The results for pure B_2O_3 are from Ref. 36. The curves have been shifted vertically, in subsequent steps of 1, for clarity.

large changes occur in the low Q range for increasing Ag_2O content [see Fig. 1(a)]. With addition of Ag_2O the large first sharp diffraction peak (FSDP) at 1.61 \AA^{-1} for B_2O_3 decreases in amplitude and splits into several smaller peaks in the range between 1.3 and 3.5 \AA^{-1} . The sharp peak at 1.32 \AA^{-1} for the $x=0.5$ (Ag) glass shows the presence of significant correlations on length scales considerably longer than for B_2O_3 . Also, Na_2O modification causes a shift of the FSDP to lower Q values [1.35 \AA^{-1} for $x=0.5$; see Fig. 1(b)], indicating an increased correlation length. It should be noted that the scattering of neutrons for all the glasses studied here is dominated by the boron-oxygen network. Thus it is the intermediate-range order of the boron-oxygen network, i.e., the relative arrangement of the BO_3/BO_4 groups, that changes substantially for the cases of Ag_2O and Na_2O modifications, whereas the intermediate-range ordering of the B-O network is little affected for the Li_2O borate glasses. In Table I the positions Q_1 and widths DQ_1 of the FSDP of the investigated glasses are summarized.

Let us now consider real-space information about the structure of the Ag_2O , Na_2O , and Li_2O modified glasses. The atomic pair correlation functions $G(r)$, obtained by Fourier transformation of the respective structure factors, are shown in Fig. 2. First we focus on the short-range order, which is determined by the range $r < 3 \text{ \AA}$. The first peak in $G(r)$, which is located at about 1.4 \AA for all the investigated glasses, is attributed to the nearest-neighbor B-O distance, and the second peak to B-B and O-O nearest-neighbor distances and possibly also to nearest M-O distances from comparison with the corresponding crystalline structures.³⁸⁻⁴¹ The positions of the peak maxima for the different glasses are given in Table II. As seen in the table, the first two peaks move only to slightly higher r values with increasing modifier content; i.e., the distances within short-range order are not much affected by Li_2O , Na_2O , or Ag_2O modifications. A slight broadening of the second peak at about 2.4 \AA is observed in the case of Ag_2O and Na_2O modifications (see below).

In Figs. 3(a) and 3(b) we show the correlation function

TABLE I. Peak positions and double half width values at half maximum (2 HWHM) for the first peak (FSDP) in the structure factors of the $x\text{Ag}_2\text{O}-\text{B}_2\text{O}_3$, $x\text{Li}_2\text{O}-\text{B}_2\text{O}_3$, and $0.5\text{Na}_2\text{O}-\text{B}_2\text{O}_3$ glasses. The half width values were measured at the low- Q side of the FSDP's.

Glass composition		Q_1 (\AA^{-1})	2 HWHM ΔQ_1 (\AA^{-1})
B_2O_3		1.61	0.59
$x\text{Li}_2\text{O}-\text{B}_2\text{O}_3$	$x=0.125$	1.60	0.58
	$x=0.25$	1.56	0.54
	$x=0.50$	1.53	0.49
$x\text{Ag}_2\text{O}-\text{B}_2\text{O}_3$	$x=0.125$	1.71	0.96
	$x=0.25$	1.35	0.46
	$x=0.50$	1.32	0.45
$0.5\text{Na}_2\text{O}-\text{B}_2\text{O}_3$		1.35	0.52

$T(r)$ expanded in the range of the first peak for the Ag_2O and Li_2O modified glasses, respectively. While the first peak for B_2O_3 can be well fitted by a Gaussian, the fit becomes worse with increasing $M_2\text{O}$ content. This is due to the fact that the peak gradually becomes more asymmetric at higher $M_2\text{O}$ contents, as seen in Figs. 3(a) and 3(b). We have, therefore, tried to fit two Gaussian peaks to the data. Excellent agreement is found for all compositions. This is perhaps not surprising in view of the additional fitting parameters. However, it is reassuring that

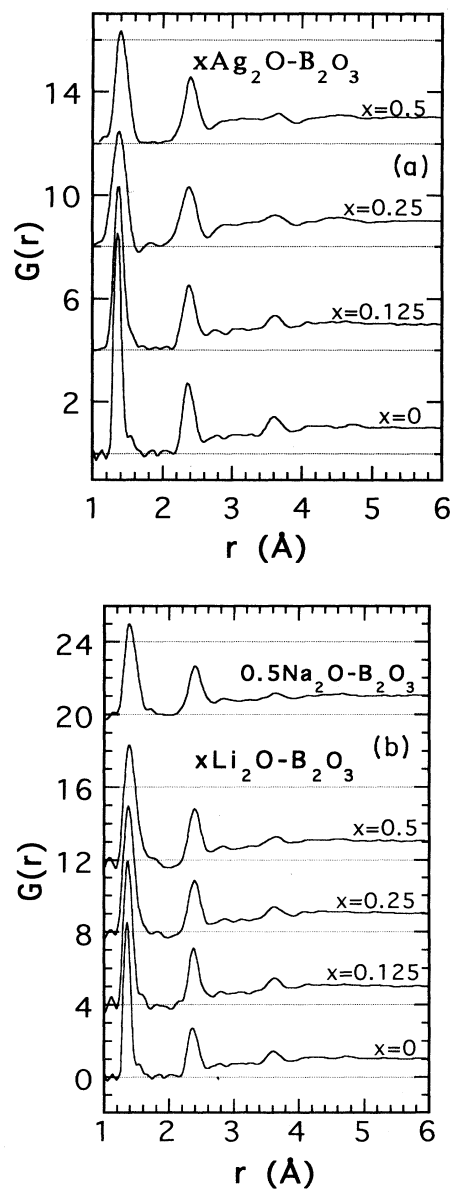


FIG. 2. Total atomic pair correlations functions $G(r)$ for (a) $x\text{Ag}_2\text{O}-\text{B}_2\text{O}_3$ and (b) $0.5\text{Na}_2\text{O}-\text{B}_2\text{O}_3$ and $x\text{Li}_2\text{O}-\text{B}_2\text{O}_3$ glasses. The results for B_2O_3 are from Ref. 36. The curves have been shifted vertically for clarity.

TABLE II. Peak positions in the pair correlation functions $G(r)$ and coordination numbers N_{B-O} calculated from the Gaussian fits of the first peak in $T(r)$ (see Fig. 3). The first peak position corresponds to the B-O distance, the second to mainly the O-O and B-B distances, the third to mainly the second B-O distance, and the fourth to mainly the third B-O distance.

Glass composition		r_1 (Å)	r_2 (Å)	r_3 (Å)	r_4 (Å)	N_{B-O}
B_2O_3		1.367	2.381	2.793	3.620	2.97
$xLi_2O-B_2O_3$	$x=0.125$	1.378	2.395	2.840	3.635	3.03
	$x=0.25$	1.387	2.405	2.850	3.635	3.15
	$x=0.50$	1.398	2.410	2.880	3.685	3.48
$xAg_2O-B_2O_3$	$x=0.125$	1.382	2.395	2.780	3.630	3.10
	$x=0.25$	1.390	2.390	2.930	3.630	3.34
	$x=0.50$	1.405	2.410	2.930	3.675	3.64
$0.5Na_2O-B_2O_3$		1.395	2.405	2.850	3.640	3.55

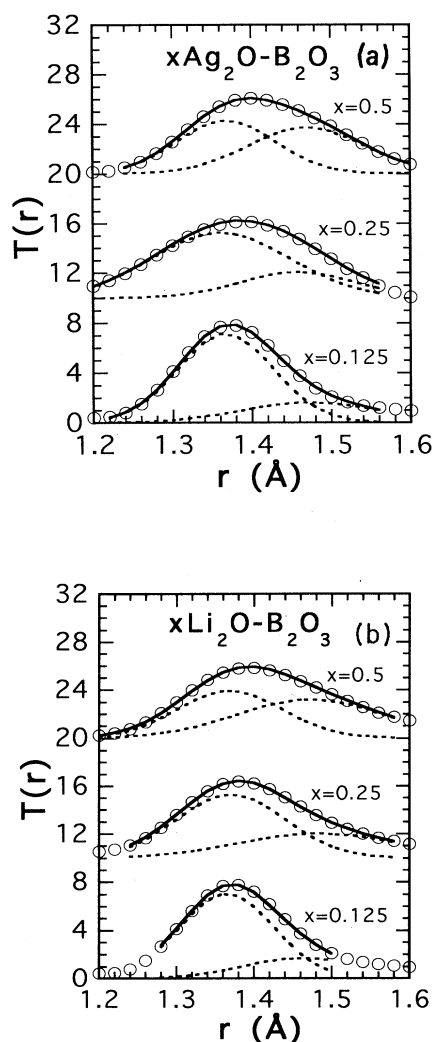


FIG. 3. Radial correlation functions $T(r)=4\pi\rho G(r)$, for (a) $xAg_2O-B_2O_3$ and (b) $xLi_2O-B_2O_3$ glasses. Solid curves represent fits of two Gaussians peaks. Dashed curves represent the individual Gaussians resulting from the fit. The curves have been shifted vertically for clarity. The low- r peak corresponds to the B-O distance in the BO_3 units (1.37 Å), and the high- r peak corresponds to the B-O distance in the BO_4 units (1.47 Å). The coordination number N_{B-O} (see Table II) and the fraction of BO_4 units (see Fig. 4) are calculated from the fit.

in all fits one of the peaks occurs at 1.37 ± 0.01 Å, i.e., the B-O distance of pure B_2O_3 , and that the width of this peak is indistinguishable from that of the resolution function. The first peak progressively decreases in intensity for increasing M_2O content, and the other peak at 1.47 ± 0.02 Å increases simultaneously in intensity. It has previously been shown that the additional oxygens, introduced with the M_2O modifications of the network, locally change the coordination of the boron atoms from 3 to 4.¹⁰⁻¹³ It is expected that the B-O distances of the formed BO_4 groups are slightly larger than those of the BO_3 groups due to the larger coordination. Thus we attribute the peak at about 1.37 Å to B-O correlations involving three-coordinated borons and the peak around 1.47 Å to correlations involving four-coordinated borons. Indeed, for the corresponding crystalline phases, the four-coordinated borons are surrounded by oxygens at several distances close to 1.47 Å.³⁸⁻⁴¹ Thus the two distances observed here are almost identical to those of the corresponding BO_3 to BO_4 groups in the crystalline compounds.³⁸⁻⁴¹ To our knowledge this is the first time two different B-O nearest-neighbor distances have been observed in a borate glass. This was possible due to the high real-space resolution resulting from the wide momentum transfer range of the measured structure factors.

The relative intensity change of the two peaks with increasing M_2O content is consistent with a progressively increasing transformation of BO_3 to BO_4 groups. This has previously been proposed from NMR,¹⁰⁻¹³ Raman-scattering,^{14,15} and infrared experiments^{11,16,17} and chemical considerations. The mean B-O coordination numbers calculated from the sum of the two peaks areas [in $J(r)=rT(r)$] are given in Table II. From the relative peak areas of the BO_3 and BO_4 peaks [see Figs. 3(a) and 3(b)], we can calculate the fraction of four-coordinated borons according to $N_{BO_4} = A_{BO_4} / (A_{BO_4} + A_{BO_3})$, where A is the area in $J(r)$ weighted by the respective neutron-scattering lengths. The results for the three compositions of Ag_2O and Li_2O modifications are shown in Fig. 4. As seen in the figure, the fraction of BO_4 units increases with increasing M_2O content. The results are almost identical for the Ag_2O and Li_2O modifications. Excellent agreement is found between our neutron results and reported NMR results¹⁰⁻¹³ (see Fig. 4) and with the fraction ex-

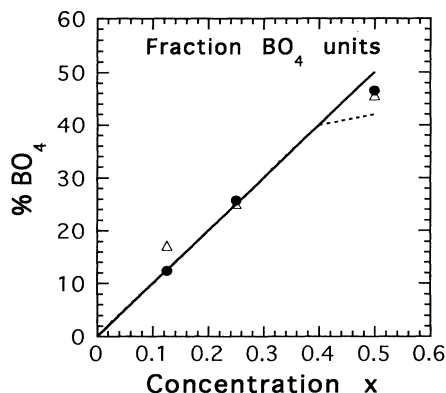


FIG. 4. Fraction of BO_4 units as a function of the network modifier concentration x : (●) $x\text{Li}_2\text{O}-\text{B}_2\text{O}_3$ and (△) $x\text{Ag}_2\text{O}-\text{B}_2\text{O}_3$. The solid line represents the number of BO_4 units with the assumption that every added oxygen produce one new BO_4 unit, and the dotted line shows a fit to NMR data obtained in Ref. 10.

pected from the assumption that one added oxygen atom coordinates to two borons. This lends support to the used fitting procedure of the first peak in $T(r)$.

A special property of the ^7Li (and thereby also of natural Li) is the negative neutron-scattering length. In the pair correlation function, which is proportional to $b_i b_j$ for a given atomic pair ij , the correlations between Li and a nucleus with a positive scattering length thus result in negative peaks in $G(r)$. A negative peak is clearly observed in the $G(r)$ for the $x\text{Li}_2\text{O}-\text{B}_2\text{O}_3$ glasses at $2.0 \pm 0.05 \text{ \AA}$ for all the samples; see Fig. 2(b). The intensity of the negative peak grows with increasing x as expected. It corresponds most likely to Li-O correlations, since Li^+ is expected to coordinate to the oxygens of the negatively charged BO_4 units. An approximate value of the average Li-O coordination number $N_{\text{Li-O}}$ is estimated from the area of the negative peak in $J(r)$ to be about 4.2 ± 0.5 for all the three samples.

By mixing appropriate amounts of ^6Li and ^7Li , it is possible to obtain a sample with zero scattering from lithium Li^0 . This is useful since the difference between the radial distribution functions of a Li^0 sample and a sample with natural lithium Li^n contains only the partial radial distribution functions involving Li, i.e., in this case Li-O, Li-B, and Li-Li, provided that the first B-O peak is scaled to the same area. We have investigated one such sample with $x=0.5$. The resulting difference in $J(r)$ between the Li^0 and Li^n samples by the first B-O peak area is shown in Fig. 5. The scaling is performed because the relative scattering cross section of the B-O correlations to the total $J(r)$ are different for the two samples. The peak of the nearest Li-O distance (which now has turned positive because of the subtraction) is again evident in the difference function. The Li-O coordination number $N_{\text{Li-O}}$ is estimated from the area of the peak (integrated in the range $1.65\text{--}2.3 \text{ \AA}$) to be about 4.1 ± 0.5 , in accordance

with the determination directly from $J(r)$. There are two additional peaks which are readily discernible at 3.0 ± 0.1 and $4.0 \pm 0.1 \text{ \AA}$. They are attributed to predominantly involve the nearest Li-B and Li-Li distances, respectively, in accordance with the crystalline structure.

We note that the short-range order is almost identical for the Li_2O , Ag_2O , and Na_2O glasses. This encourages us to apply the same procedure to the $0.5\text{Ag}_2\text{O}-\text{B}_2\text{O}_3$ and $0.5\text{Na}_2\text{O}-\text{B}_2\text{O}_3$ samples, however, using the Li^0 sample as the sample of null scattering from the cation. To reduce the B-B, B-O, and O-O correlations in the difference function, the first B-O peaks in $J(r)$ of the two samples were scaled to the same area. This should give reasonable estimates of the short-range M-O, M-B, and M-M correlations. In Fig. 5 we have also shown the difference in $J(r)$ between the $0.5\text{Ag}_2\text{O}-\text{B}_2\text{O}_3$ and $0.5\text{Na}_2\text{O}-\text{B}_2\text{O}_3$ samples, respectively, and the correspondingly scaled Li^0 sample. Three peaks can be distinguished in the two difference curves located at 2.4 ± 0.1 , 3.2 ± 0.1 , and $4.5 \pm 0.1 \text{ \AA}$ for the Ag_2O modified glass and at 2.3 ± 0.1 , 3.4 ± 0.1 , and $4.6 \pm 0.1 \text{ \AA}$ for the Na_2O modified glass. In analogy with the case of the lithium borate glass, we attribute the peaks to the first M-O, M-B, and M-M shells, respectively. The significance of the first peak in the difference function has to be carefully checked since it coincides with the second peak in the total $J(r)$ for both the $0.5\text{Ag}_2\text{O}-\text{B}_2\text{O}_3$ and $0.5\text{Na}_2\text{O}-\text{B}_2\text{O}_3$ sample. It is then

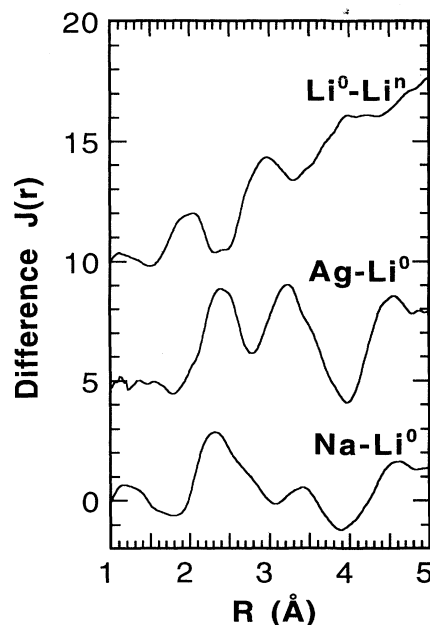


FIG. 5. Difference functions obtained from the difference between following radial distributions functions $J(r)$: $0.5\text{Li}_2\text{O}-\text{B}_2\text{O}_3$ glasses, one with a mixture of ^6Li and ^7Li to obtain zero scattering from Li and one with natural Li, $0.5\text{Ag}_2\text{O}-\text{B}_2\text{O}_3$ and $0.5\text{Li}_2\text{O}-\text{B}_2\text{O}_3$ with $\text{Li}(\sigma=0)$, and $0.5\text{Na}_2\text{O}-\text{B}_2\text{O}_3$ and $0.5\text{Li}_2\text{O}-\text{B}_2\text{O}_3$ with $\text{Li}(\sigma=0)$. The first peak (B-O) in the radial distribution functions are scaled to the same area. The curves have been shifted vertically, in subsequent steps of 5, for clarity.

reassuring to note that from EXAFS (Refs. 20 and 21) and x-ray-diffraction^{18,19} measurements the Ag-O and Na-O distances were reported to be 2.3 and 2.4 Å, respectively. The mean coordination numbers $N_{\text{Ag-O}}$ and $N_{\text{Na-O}}$ are estimated to be about 3.7 ± 0.5 and 6.0 ± 0.5 , respectively. Both values are higher than the values of about 2.0 and 5.0, respectively, reported in Refs. 18–21. However, the latter results are based on x-ray experiments which may give large systematic errors for the coordination numbers for covalent compounds containing light atoms. It should be noted that in the present study the coordination of Na is almost identical to that of the crystalline compound. Indeed, as seen in the figure, the Na-O peak is highly asymmetric indicating a distorted polyhedron like in the crystal structure. The x-ray study in Ref. 19 arrives at an almost identical asymmetry, although the obtained total coordination number is smaller. The Ag-O coordination is, on the other hand, significantly lower than that of the corresponding crystalline compound. This finding has its counterpart in a significantly lower density for the silver modified glass ($\sim 10\%$) compared to that of the corresponding crystalline phase. The differences for the Li and the Na modified compounds are smaller, which is then in accordance with the similar M-O coordinations for the glass and crystal in these cases.

Next we turn to longer-range real-space correlations. In Fig. 6 we present data for $D(r)$ in the range 3–16 Å to highlight intermediate-range correlations. It is noticeable that for Li_2O modification only small changes are observed in $D(r)$ compared with the curve for B_2O_3 . Significant peaks are observed at around 5 and 9 Å. In contrast, for the Ag_2O and Na_2O modified glasses $D(r)$ is substantially different from that of B_2O_3 in the range 4–12 Å. The oscillations in $D(r)$ are almost completely opposite to those of B_2O_3 , and significant peaks are ob-

served around 6 and 10.5 Å. Thus the structural correlations of the Ag_2O and Na_2O modified glasses extend to longer distances than those of pure B_2O_3 and Li_2O modified glasses, in accordance with the observations in $S(Q)$.

V. DISCUSSION

Most of the results presented in this study for the short-range ordering of metal-oxide modified borate glasses are in general agreement with the ideas expressed in the Krogh-Moe model,⁹ i.e., the glass structure is locally built up by the same structural units as in the corresponding crystal. Although we cannot identify the various borate groups from the neutron-diffraction data alone, the local ordering of the boron-oxygen network as well as the metal ion coordinations are very similar to those of the corresponding crystals.

Comparing glasses with different metal-oxide modifiers, we note that the short-range boron-oxygen ordering is almost identical. However, the cation coordination appears to be different for Ag^+ , Li^+ , and Na^+ . The Li-O distance is considerably closer (2.0 Å) than the Ag-O (2.4 Å) and Na-O (2.3 Å) distances. Furthermore, the coordination numbers are different, and the lithium and silver ions are approximately four-coordinated to the oxygens, whereas sodium has a considerably higher coordination number of 6. One would expect that the coordination number increases with increasing M-O distance, as it does for the Na_2O modified glass compared to the Li_2O modified glass, because of the increased space in the first-coordination shell around the cation. Thus the lower coordination number for the silver ion than for sodium indicates a larger free volume around the silver ion. This is probably due to a higher degree of covalency of the silver ion than for the alkali ions.

It is of interest to investigate whether cations coordinate between oxygens of the same negatively charged BO_4 units as was proposed in Ref. 20 or if they have a tendency to bridge between oxygens of different BO_4 units. For a symmetrical coordination of the cation between two oxygens of the same BO_4 unit, the Ag-B, Na-B, and Li-B distances are calculated to be 2.8, 2.7, and 2.3 Å, respectively, from the obtained B-O and M-O distances. These distances are clearly considerably shorter than those attributed to the M-B distances in the present investigation (3.0, 3.4, and 3.2 Å, respectively). It is to be noted that the calculated distances fall into the minima between the first two peaks of $\Delta J(r)$, showing the low probability of such a coordination. The x-ray-diffraction results reported by Licheri *et al.*¹⁸ show similar results. Therefore, we conclude that the cations do not, on average, coordinate to two oxygens of the same BO_4 unit, but rather bridge between oxygens of different BO_4 groups. This result is in contrast to an EXAFS investigation,²⁰ but in agreement with the structural model proposed in Ref. 42.

Since the cations predominantly bridge between oxygens of different BO_4 groups and the B-O network is essentially identical for glasses with different modifier cations, the larger M-O distances for Na^+ and Ag^+ lead to

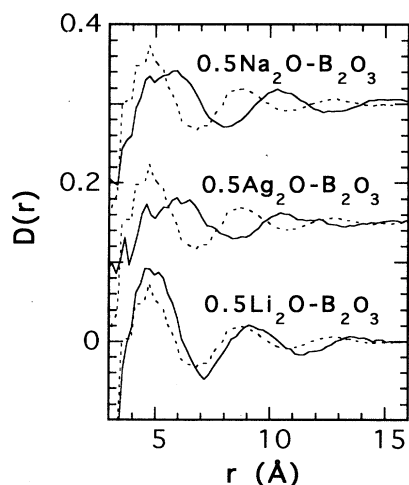


FIG. 6. Reduced radial distribution functions $D(r)$ for $0.5\text{Na}_2\text{O-B}_2\text{O}_3$, $0.5\text{Ag}_2\text{O-B}_2\text{O}_3$, and $0.5\text{Li}_2\text{O-B}_2\text{O}_3$ (solid line) compared to pure B_2O_3 (dashed line). The results for B_2O_3 are calculated from Ref. 36. The upper curves have been shifted vertically for clarity.

lower number densities for these glasses than for the corresponding lithium glasses. This in turn has to affect the intermediate-range distances, which is then expected to show up as changes in the low Q range of the structure factor, i.e., in the range of the FSDP. In this context it is also worth to note that the longer-range correlations for the Ag_2O and Na_2O modified glasses have adequate correspondence in lower network densities, and for the highest Ag_2O and Na_2O modified glasses the number densities have decreased by about 20 compared to B_2O_3 , whereas the number density of the B-O network stays approximately constant for Li_2O modification. Thus the increasing intermediate-range ordering for the Ag_2O and Na_2O modified glasses appears to be mainly due to an expansion of the boron-oxygen network caused by the introduction to the metal oxide.

A simple model for the intermediate glasses and the first sharp diffraction peak has been suggested by Moss and Price.³ It is based on the idea that molecularlike units within the network are arranged according to a dense random-packing scheme and that the orientation of these structural units is uncorrelated with their relative positions. The structural units considered are then typically cation-centered units such as SiO_4 tetrahedra for SiO_2 and BO_3 triangles for B_2O_3 . It was shown that such a model produces a FSDP which is in good agreement with experimental results for several network-forming glasses.³ A similar model for the $0.5\text{Li}_2\text{O}-\text{B}_2\text{O}_3$ glass consisting of randomly arranged BO_3 and BO_4 units has been shown by Cervinka *et al.*⁴² to be in good agreement with the experimental $S(Q)$ and in particular with the FSDP. In fact, the high- r part (above 3 Å) of the reduced radial distribution function $D(r)$ follows closely the behavior of a dense random-packing model of hard spheres with a diameter equal to that of a BO_4 unit (≈ 2.8 Å). However, for the $x\text{Ag}_2\text{O}-\text{B}_2\text{O}_3$ and $0.5\text{Na}_2\text{O}-\text{B}_2\text{O}_3$ glasses, it is obvious that such a model fails to describe the highly distorted low- Q parts of the experimental $S(Q)$ and thus the high- r part of $D(r)$. Instead, a model based on longer-range correlations between parallel diborate chain structures, similar to those observed in crystalline diborates, was proposed for the $0.5\text{Ag}_2\text{O}-\text{B}_2\text{O}_3$ glass and found to reproduce the low- Q part of the structure factor rather well.⁴² From the Ag_2O concentration dependence of the splitting of the FSDP [see Fig. 1(a)], it is clear that such a complicated structure develops with increasing Ag_2O content over the whole concentration range. The difference between the Li_2O and Ag_2O modified glasses is likely to arise from the different ionic-covalent characters of the lithium and silver ions. The silver ion has a much larger electronegativity and thus a larger tendency to form bonds with significant covalent character than the Li^+ ions.

We note that the FSDP in the highest Li_2O modified glass has a much higher intensity compared to those of the correspondingly modified silver and sodium glasses. Such a behavior was recently proposed from a void-based model for the intermediate-range structure of AX_2 network glasses.^{4,5,43} In this model it is assumed that the FSDP of covalent network glasses is a prepeak in the

concentration-concentration partial structure factor (Bhatia-Thornton formalism) due to chemical ordering of interstitial voids around cation-centered "clusters" in the structure.⁴⁴ Thus, from this model, it is expected that the intensity of the FSDP will change if voids are occupied by extrinsic atoms. An extrinsic atom with positive scattering length will reduce the contrast between the cluster and the filled void and, therefore, reduce the intensity of the FSDP, while an extrinsic atom with negative scattering length will have the opposite effect and increase the intensity of the FSDP. Such a behavior was shown for a molecular-dynamics-produced model for silica in which the voids were stuffed with various atoms. Indeed, a similar effect is shown in Fig. 7 in which the low- Q part of $S(Q)$ is shown for two $0.5\text{Li}_2\text{O}-\text{B}_2\text{O}_3$ glasses, with natural lithium Li^n (negative Li scattering length) and with Li^0 (zero Li scattering length), respectively. As seen in the figure, the FSDP of the Li^n glass is significantly stronger than for the Li^0 glass. Thus the negative scattering of Li^n enhances the intensity of the FSDP in agreement with the model in Ref. 44. Note also that the peak shifts slightly towards higher Q for the Li^0 sample. Shifts of the FSDP have therefore to be interpreted with caution since they may be caused by both the scattering lengths involved and the structural arrangements.

It is of interest to try to relate the ionic conductivities of the borate glasses to some kind of favorable structural arrangement. It is then interesting to note that the conductivities for the corresponding crystals are negligible. As shown in this study, most of the local structural arrangements of the borate glasses are strikingly similar to those of the corresponding crystals.³⁸⁻⁴¹ Hence it is unlikely that the much enhanced ionic conductivities of the glasses compared to the corresponding crystals are due to any specific local structural arrangement. Rather, the significantly lower average number density leads to a more open structure and the creation of voids and pathways within the structure in which the ionic diffusion can take place. The density difference between the crystal and glass is largest for the Ag_2O modified glasses, which

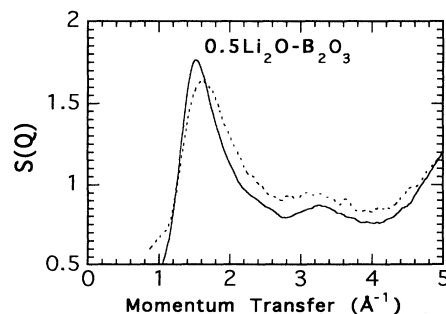


FIG. 7. Low Q range of structure factors for $0.5\text{Li}_2\text{O}-\text{B}_2\text{O}_3$ glasses with natural Li (solid curve) and with a mixture ${}^6\text{Li}$ and ${}^7\text{Li}$ to give zero scattering form lithium (dashed curve).

also show the highest ionic conductivities.

In order to obtain a further insight into the structure of the present glasses, some kind of structural modeling would be desirable. Molecular-dynamics (MD) simulations have already been performed on the Li and Ag diborate glasses⁴⁵ and compared to the neutron data for the $x = 0.5$ glasses presented here. However, it is generally hard to find a good approximation of all the pair potentials required for many component systems such as the present glasses. An alternative route is to use the reverse Monte Carlo (RMC) method,^{46,47} which makes direct use of the available experimental data without any assumption of the potentials involved. It has recently been successfully applied to other network and fast ion conducting glasses.⁴⁸ We are presently performing RMC simulations on the glasses discussed in this paper, and the results will be presented in a forthcoming report.

VI. CONCLUSION

To summarize, the structures of Ag_2O , Li_2O , and Na_2O modified borate glasses have been investigated using pulsed neutron diffraction. The boron-oxygen network structures of glasses with different cation modifiers are very similar on the short-range scale, i.e., nearest-neighbor and next-nearest-neighbor distances. A progressive change of the coordination of the boron atoms from 3 to 4 is evident from the evolution of the average coordination number and the splitting of the first B-O

distances with increasing modifier content. However, the intermediate-range structures, i.e., the relative arrangement of the various molecularlike borate groups, are different for Li_2O , Na_2O , and Ag_2O modified glasses, respectively, with considerably longer-range correlations observed for silver and sodium borate glasses. The cations coordinate to oxygens and form bridges between neighboring B-O chain segments. The coordination numbers and cation-oxygen interatomic distances are different for the differently modified glasses. The Li and Ag ions are approximately four coordinated, and Na is six coordinated. The first oxygen neighbor is considerably closer to lithium than to silver and sodium. These differences affect both the number densities of the glasses as well as the intermediate correlations of the glass.

In conclusion, the data for the short-range order of the investigated metal oxide borate glasses can well be described using the Krogh-Moe model; i.e., the microscopic structure of the glass is built up by similar structural elements as in the crystal. The disorder of the glass is then introduced predominantly beyond the first few neighbor distances, and here significant differences are observed for the variously modified glasses.

ACKNOWLEDGMENT

This work was financially supported by the Swedish Natural Sciences Research Council.

- ¹W. H. Zachariasen, *J. Am. Chem. Soc.* **54**, 3841 (1932).
- ²B. E. Warren, H. Krutter, and O. Morningstar, *J. Am. Ceram. Soc.* **19**, 202 (1936).
- ³S. C. Moss and D. L. Price, in *Physics of Disordered Materials*, edited by D. Adler, H. Fritzsche, and S. R. Ovshinsky (Plenum, New York, 1985), p. 77.
- ⁴S. R. Elliott, *Phys. Rev. Lett.* **67**, 711 (1991).
- ⁵S. R. Elliott, *J. Phys. Condens. Matter* **4**, 7661 (1992).
- ⁶I. T. Penfold and P. S. Salmon, *Phys. Rev. Lett.* **67**, 97 (1991).
- ⁷A. P. Sokolov, A. Kisliuk, M. Soltwisch, and D. Quitmann, *Phys. Rev. Lett.* **69**, 1540 (1992).
- ⁸L. Börjesson, A. K. Hassan, J. Swenson, and L. M. Torell, *Phys. Rev. Lett.* **70**, 1275 (1993).
- ⁹J. Krogh-Moe, *Phys. Chem. Glasses* **6**, 46 (1965).
- ¹⁰S. A. Feller, W. J. Dell, and P. J. Bray, *J. Non-Cryst. Solids* **15**, 21 (1982).
- ¹¹C. Chiodelli, A. Magistris, M. Villa, and J. L. Bjorkstam, *J. Non-Cryst. Solids* **51**, 143 (1982).
- ¹²K. S. Kim and P. J. Bray, *J. Nonmetals* **2**, 95 (1974).
- ¹³S. Hayashi and K. Hayamizu, *J. Non-Cryst. Solids* **11**, 214 (1989).
- ¹⁴F. Galeener, G. Lucovsky, and J. C. Mikkelsen, Jr., *Phys. Rev. B* **8**, 3983 (1980).
- ¹⁵J. Lorösch, M. Couzi, J. Pelous, R. Vacher, and A. Levasseur, *J. Non-Cryst. Solids* **69**, 1 (1984).
- ¹⁶E. I. Kamitsos, A. P. Patsis, M. A. Karakassides, and G. D. Chryssikos, *J. Non-Cryst. Solids* **126**, 52 (1990).
- ¹⁷H. L. Tuller and D. P. Button, in *Transport-Structure Relations in Fast Ion and Mixed Conductors*, edited by F. W. Poulsen, N. Hessel-Andersen, K. Clausen, S. Skaarup, and O. Toft Soerensen (Risø National Laboratory, Denmark, 1985).
- ¹⁸G. Licheri, A. Musini, G. Pashina, G. Piccaluga, G. Pinna, and A. Magistris, *J. Chem. Phys.* **85**, 500 (1986).
- ¹⁹G. Paschina, G. Piccaluga, and M. Magini, *J. Chem. Phys.* **81**, 6201 (1984).
- ²⁰G. Dalba, P. Fornasini, F. Rocca, E. Bernieri, E. Burratini, and S. Mobilio, *J. Non-Cryst. Solids* **91**, 153 (1987).
- ²¹G. Dalba, P. Fornasini, and F. Rocca, *J. Non-Cryst. Solids* **123**, 310 (1990).
- ²²C. Huang and A. N. Cormack, *J. Chem. Phys.* **93**, 8180 (1990).
- ²³G. N. Greaves, *J. Non-Cryst. Solids* **71**, 203 (1987).
- ²⁴M. C. Eckersley, P. H. Gaskell, A. C. Barnes, and P. Chieux, *Nature* **335**, 525 (1988); *ibid.* **350**, 675 (1991).
- ²⁵C. A. Angell, *Solid State Ion.* **18/19**, 72 (1986); *Annu. Rev. Phys. Chem.* **43**, 693 (1992).
- ²⁶M. D. Ingram, *Phys. Chem. Glasses* **28**, 215 (1987).
- ²⁷W. Soppe, J. Kleerebezem, and H. W. den Hartog, *J. Non-Cryst. Solids* **93**, 142 (1987).
- ²⁸M. P. Malugani and R. Mercier, *Solid State Ion.* **13**, 293 (1984).
- ²⁹C. Carini, M. Cutroni, A. Fontana, G. Mariotto, and F. Rocca, *Phys. Rev. B* **29**, 3567 (1984).
- ³⁰T. Minami, *J. Non-Cryst. Solids* **73**, 273 (1985).
- ³¹G. Placzek, *Phys. Rev.* **86**, 377 (1952).
- ³²L. Börjesson, *Phys. Rev. B* **36**, 4600 (1987).
- ³³L. Börjesson and L. M. Torell, *Solid State Ion.* **25**, 85 (1987).
- ³⁴W. S. Howells (unpublished).
- ³⁵M. Howe, W. S. Howells, and R. L. McGreevy, *J. Phys. Condens. Matter* **1**, 3433 (1989).
- ³⁶P. A. V. Johnson, A. C. Wright, and R. N. Sinclair, *J. Non-Cryst. Solids* **50**, 281 (1982).
- ³⁷A. C. Wright, A. G. Claire, D. I. Grimley, and R. N. Sinclair,

- J. Non-Cryst. Solids **112**, 33 (1989).
- ³⁸J. Krogh-Moe, *Acta Crystallogr.* **15**, 190 (1962).
- ³⁹J. Krogh-Moe, *Acta Crystallogr. B* **24**, 179 (1968).
- ⁴⁰J. Krogh-Moe, *Acta Crystallogr.* **18**, 77 (1965).
- ⁴¹J. Krogh-Moe, *Acta Crystallogr. B* **30**, 578 (1974).
- ⁴²L. Cervinka, F. Rocca, P. Fornasini, and G. Dalba, *J. Non-Cryst. Solids* **150**, 140 (1992).
- ⁴³J. H. Lee and S. R. Elliott, *Phys. Rev. B* **50**, 5981 (1994).
- ⁴⁴A. B. Bhatia and D. E. Thornton, *Phys. Rev. B* **2**, 3004 (1970).
- ⁴⁵M. C. Abramo, G. Pizimenti, and A. Consola, *Philos. Mag. B* **64**, 495 (1991).
- ⁴⁶R. L. McGreevy and L. Pusztai, *Mol. Sim.* **1**, 359 (1988).
- ⁴⁷D. A. Keen and R. L. McGreevy, *Nature* **344**, 423 (1990).
- ⁴⁸J. Wicks, L. Börjesson, R. L. McGreevy, W. S. Howells, and G. Bushnell-Wye, *Phys. Rev. Lett.* **74**, 726 (1995).